

# Exact computation of the mean velocity, molecular diffusivity and dispersivity of a particle moving on a periodic lattice

Kevin D. Dorfman\*

*Institut Curie, Physico-Chimie/UMR 168,  
26 Rue d'Ulm, 75248 Paris Cedex 5, France*

(Dated: November 21, 2018)

## Abstract

A straightforward analytical scheme is proposed for computing the long-time, asymptotic mean velocity and dispersivity (effective diffusivity) of a particle undergoing a discrete biased random walk on a periodic lattice amongst an array of immobile, impenetrable obstacles. The results of this Taylor-Aris dispersion-based theory are exact, at least in an asymptotic sense, and furnish an analytical alternative to conventional numerical lattice Monte Carlo simulation techniques. Results obtained for an obstacle-free lattice are employed to establish generic relationships between the transition probabilities, lattice size and jump time. As an example, the dispersivity is computed for a solute moving through an isotropic array of obstacles under the influence of a finite external field. The calculation scheme is also shown to agree with existing zero-field results, the latter obtained elsewhere either by first-passage time analysis or use of the Nernst-Einstein equation in the zero-field limit. The generality of this scheme permits the study of more complex lattice structures, in particular trapping geometries.

PACS numbers: 05.40.Jc, 87.15.Tt, 02.70.Ss

---

\*Electronic address: Kevin.Dorfman@curie.fr

## I. INTRODUCTION

Lattice Monte Carlo simulation constitutes a powerful method for computing the average transport rates of a particle moving through a fixed network of obstacles by modeling the continuous transport process as a discrete random walk, biased or unbiased, across a lattice. At the heart of this technique lies a master equation [1] which quantifies the probability of jumping from one point on the lattice to an adjacent point in a given period of time. Owing to the stochastic (probabilistic) nature of the master equation, computer simulations based upon lattice Monte Carlo techniques require numerous realizations of the system in order to yield statistically significant results. Moreover, since average transport rates are valid only for long times, each simulation must be sufficiently long in order to satisfy this criteria.

Gel electrophoresis is one particularly relevant application of lattice Monte Carlo techniques, where the fibers of the gel are modeled as obstacles in the network which “reject” solute jumps onto them as a result of hard-core repulsion forces. In a recent series of publications [2, 3, 4, 5, 6, 7, 8, 9, 10], Slater and coworkers invoked lattice Monte Carlo-type schemes to compute the effective solute mobility,  $\bar{M}^*$ , for transport in spatially periodic model gels in the “Ogston-sieving” regime of gel electrophoresis. The latter works are unique in that they do not rely upon computer simulations at all. Rather, analytical solutions are obtained for the solute mobility, based upon the fact that, for periodic lattices, unit-cell probabilities can be computed analytically in the long-time (steady-state) limit. As a consequence, Slater and coworkers have been able to consider a vast array of periodic model gels, both 2-D and 3-D, thereby critically assessing the validity of existing gel electrophoresis theories and investigating the effects of gel structure on the resultant average solute mobility. Results obtained from these types of calculations are presumably exact, at least in an asymptotic sense, for perfectly periodic structures, such as those which may be realized in microfluidic environments [11, 12, 13]. Results for pseudo-random structures, which may be more representative of real gels, can be obtained by repeating the periodic calculation scheme numerous times in conjunction with random samplings of possible obstacle configurations (using the spatial periodicity to mimic macroscopic-sized gels), and then averaging the ensemble of results [4, 14]. The efficiency of analytical methods renders such calculations very feasible.

Although the aforementioned series of papers [2, 3, 4, 5, 6, 7, 8, 9, 10] has made significant progress in addressing the issue of the average solute mobility (or, equivalently, the mean

solute velocity,  $\bar{\mathbf{U}}^*$ ), much less progress has been made towards calculating solute *dispersion* arising as a result of the stochastic nature of the transport on the lattice. In the context of separation sciences [15], it is essential to quantify both the dispersion and the average mobility, since the relative mobility of the particles being separated determines the degree of the separation, while the dispersion governs the separation sharpness. Moreover, while the local solute mobility dyadic,  $\mathbf{M}$ , and diffusivity dyadic,  $\mathbf{D}$ , are related at each point in space by the Stokes-Einstein equation [24],

$$\mathbf{D} = \mathbf{M}kT, \quad (1.1)$$

with  $kT$  the Boltzmann factor, the comparable Nernst-Einstein relationship between the dispersivity dyadic,  $\bar{\mathbf{D}}^*$ , and the average mobility dyadic,  $\bar{\mathbf{M}}^*$ ,

$$\bar{\mathbf{D}}^* = \bar{\mathbf{M}}^*kT, \quad (1.2)$$

is only valid in the limit of vanishingly small applied fields.

Mercier *et al.* [16] exploited this property of eq. (1.2) to successively compute the components of  $\bar{\mathbf{D}}^*$  in the zero-field limit [25]. Explicitly, an analytical scheme [2] was invoked to compute the different mean velocity vectors, say,  $\bar{\mathbf{U}}_x^*$  and  $\bar{\mathbf{U}}_y^*$ , corresponding to infinitesimally small forces being applied in the subscripted spatial directions. The average mobility was then obtained by using the linear relationship,

$$\bar{\mathbf{U}}^* = \bar{\mathbf{M}}^* \cdot \mathbf{F}, \quad (1.3)$$

in conjunction with each of the mean velocities. The resulting average mobility tensor proves to be independent of field strength, whereupon eq. (1.2) immediately furnishes the dispersivity dyadic,  $\bar{\mathbf{D}}^*$ . The resulting dispersivity was shown to agree exactly with that obtained by first-passage time analysis [16]. Given the relative ease of the mobility calculation compared to its first-passage time counterpart, Mercier *et al.* advocate the use of the former.

While calculating the dispersion (effective diffusion) coefficient for an unbiased random walk on the lattice is clearly a non-trivial endeavor, this is the limiting case of the much broader problem of dispersion occurring during *biased* random walks, the bias being induced by the presence of finite electric fields (or some other external force) [26]. Keller *et al.* [17] recently proposed a method for computing the dispersivity dyadic from biased lattice walks in the low-field limit, based upon what is essentially a volume-averaging scheme. In §VIB,

we will demonstrate that, in contrast to the present theory, the latter volume-averaged scheme does not furnish the correct effective diffusivity for the anisotropic array discussed above [16]. While this does not address the underlying validity (or lack thereof) of the volume-averaged approach, it does bring into question its applicability to the present class of problems. Consequently, no simple method exists in the literature for computing solute dispersion from a generic lattice model, and it has been noted [10] that such a calculation scheme would be extremely useful for analyzing trapping-based separations.

The present contribution addresses this need by developing an asymptotically exact, analytical scheme for computing the mean velocity vector,  $\bar{\mathbf{U}}^*$ , and dispersivity dyadic,  $\bar{\mathbf{D}}^*$ , from lattice Monte Carlo models, by way of discrete generalized Taylor-Aris dispersion theory for spatially periodic networks [18, 19]. The latter theory was initially developed as a means to compute  $\bar{\mathbf{U}}^*$  and  $\bar{\mathbf{D}}^*$  from lumped-parameter models of transport in model porous media [18] and microfluidic networks [19]. We will show that the lattice random walk has much in common with the existing lumped-parameter transport problem, whereupon the moment scheme invoked previously [18, 19] may be readily employed here to homogenize the master equation governing transport on the periodic lattice. Consideration of the obstacle-free case furnishes generic relationships between the jump time, transition probabilities and the lattice spacing. These generic relationships between the parameters are used in an illustrative example of a solute moving on a simple periodic lattice in the presence of a finite external field. The theory simplifies substantially in the absence of a field, leading to a compact scheme for computing the effective diffusion coefficient. The simplified theory is invoked to compute the zero-field dispersion coefficients for the asymmetric lattice problem originally considered by Mercier *et al.* [16], demonstrating that the present theory successfully reproduces their results.

## II. BIASED RANDOM WALK ON A PERIODIC LATTICE

### A. Geometry

Consider a periodic lattice of the type depicted in Fig. 1. The available sites of the lattice are indicated by white boxes and the unavailable sites, corresponding to the obstacles in the array, are indicated by black boxes. Transport between lattice sites occurs by discrete

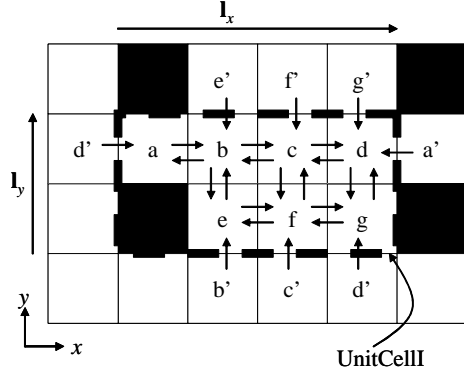


FIG. 1: Basic graph,  $\Gamma_b$ , of a periodic lattice with an asymmetric array of obstacles. The nodes of the graph are indicated by the lettered white boxes ( $a-g$ ), and the edges of the graph are indicated by the arrows. The periodic unit cell is indicated by the heavy dashed line, and those nodes with a prime affix correspond to homologous vertices lying outside the unit cell. Base lattice vectors  $\mathbf{l}_x$  and  $\mathbf{l}_y$  are indicated. Only those edges entering the unit cell are included in the basic graph. Diffusion in this particular array was previously considered in Ref. 16.

“jumps” between them. The spatial periodicity of the lattice is reflected by the presence of a repetitive unit cell, which reproduces the entire unbounded medium upon translation by its base lattice vectors ( $\mathbf{l}_1, \mathbf{l}_2, \mathbf{l}_3$ ). Each cell is characterized by its respective discrete location vector,  $\mathbf{I} = (I_1, I_2, I_3)$ , with the origin arbitrarily chosen to be located at the cell  $\mathbf{I}_0 = \mathbf{0}$ . The position of the locator point, say, the centroid, of cell  $\mathbf{I}$  is given by the discrete vector  $\mathbf{R}_\mathbf{I} = I_1\mathbf{l}_1 + I_2\mathbf{l}_2 + I_3\mathbf{l}_3$ .

The unbounded, periodic lattice may be represented by a series of three graphs (although only the unit-cell based local graph,  $\Gamma_l$ , will be necessary for computing  $\bar{\mathbf{U}}^*$  and  $\bar{\mathbf{D}}^*$ ), where the nodes of the graph correspond to the lattice sites and the edges of the graph correspond to the possible jumps between sites. The specifics of the graphical construction are discussed at length in Ref. 19, whereupon the following exposition will be brief. Each lattice site (node) is assigned a discrete location  $(\mathbf{I}, i)$ , where  $i$  represents the intracellular position (i.e.  $a-g$  in Fig. 1). As a consequence of the spatial periodicity of the network, it only proves necessary to consider edges of the type indicated in Fig. 1. Let  $\Omega^+(i)$  be the subset of the edges  $j$  entering node  $(\mathbf{I}, i)$  from node  $(\mathbf{I}', i')$ , and  $\Omega^-(i)$  be those edges exiting node  $(\mathbf{I}, i)$  and entering node  $(\mathbf{I}', i')$  [27]. The global graph,  $\Gamma_g$ , contains all of the infinitely many nodes and all of the edges connecting them, equipollent with the unbounded lattice. As an

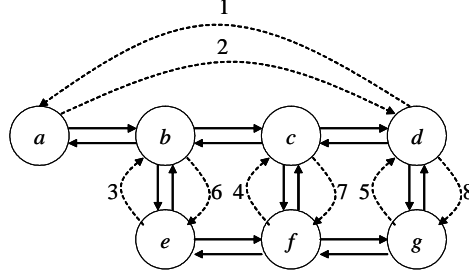


FIG. 2: The local graph,  $\Gamma_l$ , constructed from the basic graph of Fig. 1. Those edges with non-zero macroscopic jump vectors  $\mathbf{R}(j)$  are indicated by the dashed lines. Edge numbers refer to the calculation of §VIB.

intermediate step, we construct the basic graph,  $\Gamma_b$ , depicted in Fig. 1, which includes: (i) all of the nodes in the unit cell; (ii) all those edges contained wholly within the unit cell; (iii) those edges *entering* the unit cell; and (iv) their associated homologous vertices, the latter indicated with the prime affix in Fig. 1.

A macroscopic jump vector,

$$\mathbf{R}(j) = \mathbf{R}_{\mathbf{I}} - \mathbf{R}_{\mathbf{I}'}, \quad (2.1)$$

is assigned to each of the edges, this vector being identically zero for those edges which do not cross the boundary of the unit cell. This permits one to distinguish between edges connecting, say,  $e' \rightarrow b$  and  $e \rightarrow b$  in the basic graph, since their respective macroscopic jump vectors are  $\mathbf{R} = -\mathbf{1}_y$  and  $\mathbf{R} = \mathbf{0}$ . Use of the macroscopic jump vectors prevents some (potentially significant) geometrical simplifications achieved in the lattice models proposed by Slater and coworkers [2, 3], since “identical” sites in their model now typically differ with respect to the macroscopic jump vectors in  $\Omega^+(i)$ . Since the velocity may be computed without use of these vectors [cf. eq. (3.9)], their scheme [3] for computing  $\bar{\mathbf{U}}^*$  is more efficient for certain geometries. However, the primary contribution here is a scheme for computing  $\bar{\mathbf{D}}^*$  [cf. eq. (3.10)], which requires using the macroscopic jump vectors to compute the moments of the probability [cf. eq. (3.1)].

The local graph,  $\Gamma_l$ , depicted in Fig. 2, is constructed by combining the homologous vertices on  $\Gamma_b$  and contracting those edges between them. The dashed lines in Fig. 2 correspond to edges which cross the boundary of the unit cell in the basic graph (and thus have non-zero macroscopic jump vectors). Reference to the discrete position vector  $\mathbf{I}$  is no longer necessary in the local graph, since the periodic structure of the medium has been

embedded in the macroscopic jump vectors.

## B. Master Equation

Consider the probability  $P(\mathbf{I}, i, N | \mathbf{I}_0, i_0, 0)$  that the particle will be located at site  $(\mathbf{I}, i)$  on  $\Gamma_g$  at step  $N$ , given its initial location at site  $(\mathbf{I}_0, i_0)$ . In the usual manner [19], the final results only depend upon the displacement,  $\mathbf{I} - \mathbf{I}_0$ , from the arbitrarily positioned origin. In light of the prior choice  $\mathbf{I}_0 = \mathbf{0}$ , the probability adopts the canonical form  $P \equiv P(\mathbf{I}, i, N | i_0)$ .

During each time step of duration  $\tau$ , a particle located at a node adjacent to node  $i$ , say, node  $i'$ , may enter node  $i$  via a jump through an edge in  $\Omega^+(i)$ . If the particle is located at node  $i$ , it may either remain there, say, due to a rejected jump caused by the presence of an obstacle, or exit through one of the edges contained in  $\Omega^-(i)$ . For each edge  $j$ , denote the transition probability  $w(j)$  that a particle located at the initial vertex of edge  $j$  will chose to move through that edge during time  $\tau$ , and for each node  $i$ , let  $w(i)$  denote the probability that the particle will chose to remain at node  $i$  during time  $\tau$ . Since a particle located at node  $i$  must either remain there or exit therefrom at each time step, there exists the conservation relationship [28]:

$$w(i) + \sum_{j \in \Omega^-(i)} w(j) = 1 \quad (\forall i). \quad (2.2)$$

The evolution of  $P$  is governed by the following master equation quantifying the change in probability at each node on the global graph,  $\Gamma_g$ , between time step  $N$  and  $N + 1$ :

$$\begin{aligned} P(\mathbf{I}, i, N + 1) - P(\mathbf{I}, i, N) = & \sum_{j \in \Omega^+(i)} w(j)P(\mathbf{I}', i', N) \\ & - [1 - w(i)]P(\mathbf{I}, i, N) \\ & + \delta(\mathbf{I}, \mathbf{0})\delta(i, i_0) \times \\ & \times \delta(N, 0), \end{aligned} \quad (2.3)$$

where the dependence upon the initial condition  $i_0$  has been suppressed, and the  $\delta(i, j)$  are Kronecker delta functions;  $\delta(i, j) = 1$  if  $i = j$ ,  $\delta(i, j) = 0$  otherwise.

A rate equation may be obtained by dividing eq. (2.3) by the jump time,  $\tau$ . Interest here is focused upon the asymptotic, long-time behavior of  $P$  after many jumps ( $N \gg 1$ ), whence, to a good approximation [29],

$$\frac{P(\mathbf{I}, i, N + 1) - P(\mathbf{I}, i, N)}{\tau} \approx \frac{dP(\mathbf{I}, i, N)}{dt}. \quad (2.4)$$

The time,  $t \equiv N\tau$ , is viewed as an essentially continuous variable for the case  $N \gg 1$ , which is equivalent to the long-time limit in conventional Taylor-Aris dispersion theory [19]. Use of the latter in eq. (2.3) furnishes the following differential algebraic equation

$$\begin{aligned} \frac{dP(\mathbf{I}, i, N)}{dt} = & \sum_{j \in \Omega^+(i)} \left[ \frac{w(j)}{\tau} \right] P(\mathbf{I}', i', N) \\ & - \left[ \frac{1 - w(i)}{\tau} \right] P(\mathbf{I}, i, N) \\ & + \tau^{-1} \delta(\mathbf{I}) \delta(i, i_0) \delta(N). \end{aligned} \quad (2.5)$$

### III. MOMENT SCHEME

The master equation (2.5) possesses a mathematical structure similar to the governing equation appearing in Ref. 19, albeit with a significantly different physical interpretation. Consequently, the moment-matching scheme employed previously may be invoked here to compute the mean velocity vector,  $\bar{\mathbf{U}}^*$ , and dispersivity dyadic,  $\bar{\mathbf{D}}^*$ , for the lattice transport problem defined by eq. (2.5). The scheme is outlined in what follows, and the reader is referred to Ref. 19 for further details.

Define the local moment of the probability as the  $m$ -adic,

$$\mathbf{P}_m(i, N | i_0) \stackrel{\text{def.}}{=} \sum_{\mathbf{I}} (\mathbf{R}_{\mathbf{I}})^m P(\mathbf{I}, i, N | i_0), \quad (3.1)$$

where  $(\mathbf{R}_{\mathbf{I}})^m \equiv \mathbf{R}_{\mathbf{I}} \mathbf{R}_{\mathbf{I}} \cdots \mathbf{R}_{\mathbf{I}}$  ( $m$  times) and the sum over  $\mathbf{I}$  represent the sum over all cells. (The spatial location of cell  $\mathbf{I}_0 = \mathbf{0}$  is  $\mathbf{R}_{\mathbf{I}_0} = \mathbf{0}$ .) The total moments of the probability are the  $m$ -adics,

$$\mathbf{M}_m(N | i_0) \stackrel{\text{def.}}{=} \sum_{i \in VT_l} \mathbf{P}_m(i, N | i_0), \quad (3.2)$$

where  $VT_l$  are the vertices of the local graph. The zeroth moment is trivial,

$$M_0 = 1, \quad (3.3)$$

which reflects the conservation of the probability on the lattice. The next two higher-order total moments are expected to grow linearly with time, and possess the respective forms:

$$\frac{d\mathbf{M}_1}{dt} \approx \bar{\mathbf{U}}^*, \quad (3.4)$$

$$\frac{d}{dt} (\mathbf{M}_2 - \mathbf{M}_1 \mathbf{M}_1) \approx 2\bar{\mathbf{D}}^*. \quad (3.5)$$

We briefly outline here the moment-matching scheme [19] for computing  $\bar{\mathbf{U}}^*$  and  $\bar{\mathbf{D}}^*$ : (i) form the equations governing the local moments from eqs. (2.5) and (3.1); (ii) compute the asymptotic solutions to the first two local moments; (iii) form asymptotic total moments from the latter result and eq. (3.2); and (iv) match the asymptotic moments of the exact solution to eqs. (3.4)-(3.5). Only the results of the moment scheme will be presented, since the mathematical manipulations required to arrive at these results are lengthy and follow a procedure identical to that appearing elsewhere [19].

### A. Mean Velocity Vector

The mean velocity vector is computed by forming the sum

$$\bar{\mathbf{U}}^* = \sum_{j \in E\Gamma_l, j \in \Omega^+} \left[ \frac{w(j)}{\tau} \right] \mathbf{R}(j) P_0^\infty(i'), \quad (3.6)$$

where  $E\Gamma_l$  are the edges of the local graph, and the index  $i'$  refers to the initial vertex of edge  $j$ . The vertex field  $P_0^\infty(i)$ , corresponding to the asymptotic, steady-state probability of locating the particle at node  $i$  in the unit cell, is the solution of the linear set of equations,

$$\sum_{j \in \Omega^+(i)} w(j) P_0^\infty(i') - [1 - w(i)] P_0^\infty(i) = 0. \quad (3.7)$$

The latter are not linearly independent, and must be supplemented by the normalization condition

$$\sum_{i \in V\Gamma_l} P_0^\infty(i) = 1. \quad (3.8)$$

The present method of computing  $\bar{\mathbf{U}}^*$  differs somewhat from that employed by Slater and coworkers (see, for example, Ref. 2). In the latter, the mean velocity is computed by first solving eqs. (3.7)-(3.8) for  $P_0^\infty(i)$ . The velocity vector for each lattice site, say,  $\mathbf{v}(i)$ , is then defined as the difference in transition probability between taking a forward step and a backwards step at site  $i$ , each step being weighted by its respective displacement (i.e. zero displacement for rejected jumps). The mean velocity is then computed by the sum

$$\bar{\mathbf{U}}^* = \sum_{i \in V\Gamma_l} \mathbf{v}(i) P_0^\infty(i). \quad (3.9)$$

Equations (3.6) and (3.9) furnish identical values for  $\bar{\mathbf{U}}^*$ , since the difference between these two methods is simply a manifestation of Gauss' divergence theorem in a discrete sense; eq. (3.6) is the "surface" term and eq. (3.9) is the "volume" term.

## B. Dispersivity Dyadic

The dispersivity dyadic is computed by the edge-sum

$$\bar{\mathbf{D}}^* = \frac{1}{2} \sum_{j \in E\Gamma_l, j \in \Omega^+} \left[ \frac{w(j)}{\tau} \right] P_0^\infty(i') \tilde{\mathbf{b}}(j) \tilde{\mathbf{b}}(j), \quad (3.10)$$

wherein

$$\tilde{\mathbf{b}}(j) \stackrel{\text{def.}}{=} \mathbf{R}(j) - \mathbf{B}(i) + \mathbf{B}(i'), \quad j = \{i', i\} \quad (3.11)$$

for an edge directed from  $i'$  to  $i$ . The node-based vectors  $\mathbf{B}(i)$  are the solutions of

$$\begin{aligned} \sum_{j \in \Omega^+(i)} \left[ \frac{w(j)}{\tau} \right] P_0^\infty(i') [\mathbf{B}(i') + \mathbf{R}(j)] \\ - \left[ \frac{1 - w(i)}{\tau} \right] P_0^\infty(i) \mathbf{B}(i) \\ = P_0^\infty(i) \mathbf{U}^*. \end{aligned} \quad (3.12)$$

Equations (3.12) only define the  $\mathbf{B}$  vectors to within an arbitrary, additive constant vector. Consequently, this degree of freedom may be employed to set the  $\mathbf{B}$  vector at one of the nodes, say  $i^*$ , equal to zero,  $\mathbf{B}(i^*) = \mathbf{0}$ .

## IV. OBSTACLE-FREE CASE

Up to this point, no restrictions were placed upon the transition probabilities,  $w(j)$ , the lattice spacing,  $l$ , or the jump time,  $\tau$ , aside from the conservation statement (2.2), which ensures that the particle makes a decision (either to jump to a new site or remain at the present site) during each time step. However, by considering the trivial case of transport on an obstacle-free lattice, additional relationships may be derived between the latter parameters, at least for the case of square lattices.

Attention is restricted here to a two dimensional lattice, whose basic graph is depicted in Fig. 3, since generalizations to other dimensions are trivial. In the present circumstances, it only proves necessary to consider the case where the force is directed in a single direction on the lattice, say, the  $x$ -direction, since the spatial orientation of the lattice is arbitrary. The unit cell consists of a single node with four entering edges, each of the latter possessing the transition probability  $w_{+x}$ ,  $w_{-x}$  or  $w_y$ , depending on the edge orientation.

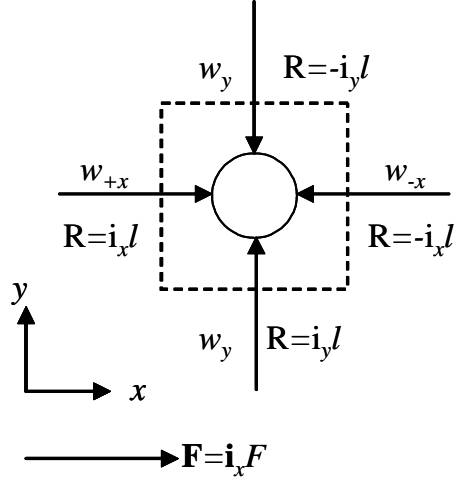


FIG. 3: Basic graph (unit cell) for a lattice in the absence of obstacles. The transition probabilities,  $w(j)$ , and macroscopic jump vectors,  $\mathbf{R}(j)$  are indicated in the figure. There are no rejected jumps, whereupon  $w(i) = 0$ . A force of magnitude  $F$  is applied in the positive  $x$ -direction.

The governing equations (3.7)-(3.8) and (3.12) are satisfied here by the trivial solutions  $P_0^\infty = 1$  and  $\mathbf{B} = \mathbf{0}$  [whereupon  $\tilde{\mathbf{b}}(j) = \mathbf{R}(j)$ ]. From eq. (3.6), the mean velocity adopts the form

$$\bar{\mathbf{U}}^* = \mathbf{i}_x (w_{+x} - w_{-x}) \frac{l}{\tau}, \quad (4.1)$$

and, from eq. (3.10), the dispersivity dyadic is

$$\bar{\mathbf{D}}^* = \mathbf{i}_x \mathbf{i}_x \left[ (w_{+x} + w_{-x}) \frac{l^2}{2\tau} \right] + \mathbf{i}_y \mathbf{i}_y \left( w_y \frac{l^2}{\tau} \right). \quad (4.2)$$

For this trivial problem, though, the proper results are known *a priori*, namely  $\bar{\mathbf{U}}^* = M\mathbf{F}$ , where  $M$  is the free solution mobility and  $\mathbf{F} = \mathbf{i}_x F$  is the applied force, and  $\bar{\mathbf{D}} = \mathbf{I}D$ , where  $D$  is the molecular diffusivity and  $\mathbf{I}$  is the idemfactor. As a consequence, the usual velocity restriction [20] is recovered,

$$(w_{+x} - w_{-x}) \frac{l}{\tau} = MF, \quad (4.3)$$

along with two restrictions governing the diffusive behavior,

$$(w_{+x} + w_{-x}) \frac{l^2}{2\tau} = \frac{w_y l^2}{\tau} = D. \quad (4.4)$$

It is our contention that the latter restrictions (4.3)-(4.4) must be satisfied by any Monte Carlo algorithm of this type, in order for the moments of the master equation to properly

reflect the microscale physics. For example, Gauthier and Slater [10] noted that their high-field Monte Carlo algorithm, which furnishes the correct velocity (4.3), predicts that the obstacle-free diffusivity depends upon the field strength. Indeed, it is readily confirmed that their choices of transition probabilities (and  $\tau$ ) fail to satisfy eq. (4.4). Consequently, the criteria of eq. (4.4) serves as a litmus test for newly proposed algorithms.

If the following normalization condition is enforced,

$$w_{+x} + w_{-x} + 2w_y = 1, \quad (4.5)$$

then eqs. (4.3)-(4.5) constitute 4 equations for 5 unknowns. If the lattice spacing,  $l$ , is left as an adjustable parameter, then one recovers the usual “small-bias” algorithm (see, for example, Ref. 2)

$$w_{\pm x} = \frac{1 \pm \epsilon}{4}, \quad w_y = \frac{1}{4}, \quad \tau = \frac{l^2}{4D}, \quad (4.6)$$

where  $\epsilon$  is the reduced field,

$$\epsilon \stackrel{\text{def.}}{=} \frac{Fl}{2kT}. \quad (4.7)$$

Remarkably, the latter results were derived solely from considering the obstacle-free velocity and diffusion coefficient, along with the normalization condition (4.5), without ever explicitly stating that  $\epsilon \ll 1$ . However, the transition probabilities are only sensible in the latter limit, or at least for the inequality  $\epsilon < 1$ , since the physical interpretation of a negative transition probability is suspect.

## V. TRANSPORT ON AN ISOTROPIC LATTICE IN A FINITE EXTERNAL FIELD

In the following illustrative example, we analyze transport occurring in a simple isotropic system, depicted in Fig. 4, under the influence of a finite field. The lattice, consisting of square obstacles of size  $l$  separated by a distance  $l$ , constitutes the simplest configuration for demonstrating the present scheme.

In the parlance of the present theory, and with the edge numbering depicted in Fig. 4, the transition probabilities are  $w(j) = w_{+x}$  for  $(j = 1, 2)$ ,  $w(j) = w_{-x}$  for  $(j = 3, 4)$ , and  $w(j) = w_y$  otherwise. For now, the specific forms of the transition probabilities,  $w(j)$ , and the jump time,  $\tau$ , will be left unspecified, although subject to the generic physical restrictions (4.3)-(4.4). As a consequence of rejected jumps, the probabilities of remaining

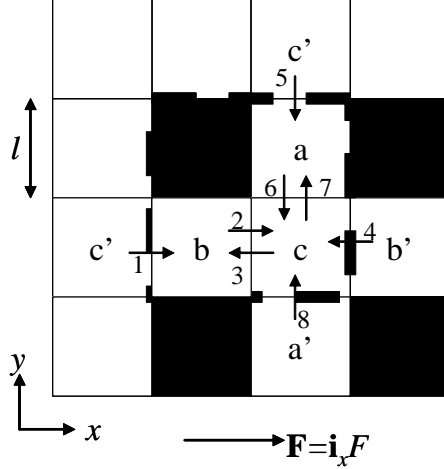


FIG. 4: Isotropic array of square obstacles of characteristic length  $l$  separated by a distance  $l$ . The repetitive unit cell is indicated by the dashed lines. An external force of strength  $F$  is applied in the  $x$ -direction to animate the particle. The labeled lattice sites and indicated arrows constitute the basic graph,  $\Gamma_b$ .

at the different lattice sites are  $w(a) = w_{+x} + w_{-x}$ ,  $w(b) = 2w_y$  and  $w(c) = 0$ . The problem specification is completed by the macroscopic jump vectors,

$$\mathbf{R}(j) = 2l \begin{cases} \mathbf{i}_x, & j = 1, \\ -\mathbf{i}_x, & j = 4, \\ -\mathbf{i}_y, & j = 5, \\ \mathbf{i}_y, & j = 8, \\ \mathbf{0}, & \text{otherwise.} \end{cases} \quad (5.1)$$

It is readily apparent that the solution  $P_0^\infty = 1/3$  satisfies eqs. (3.7)-(3.8), a consequence of the isotropy of the lattice. Substituting the relevant parameters into eq. (3.6) furnishes the mean velocity,

$$\bar{\mathbf{U}}^* = \frac{2}{3} (w_{+x} - w_{-x}) \frac{l}{\tau} \mathbf{i}_x, \quad (5.2)$$

which, with use of eq. (4.3), adopts the form

$$\bar{\mathbf{U}}^* = \frac{2}{3} M \mathbf{F}. \quad (5.3)$$

The latter result is invariant to the (arbitrary) choice of axis labels, whereupon it is recognized that isotropy of the lattice geometry renders the mean mobility tensor isotropic,

$$\bar{\mathbf{M}}^* = \mathbf{I}\bar{M}^*, \quad \bar{M}^* = \frac{2}{3}M. \quad (5.4)$$

The effective mobility,  $\bar{M}^*$ , is less than the free solution value,  $M$ , owing to the inability to make forward jumps on lattice site  $a$ . The latter observation, as well as the equivalence of eqs. (3.6) and (3.9), is rendered transparent by this considering the local velocity [3] at each node,

$$\mathbf{v}(i) = \begin{cases} M\mathbf{F}, & i = b, c, \\ \mathbf{0}, & i = a. \end{cases} \quad (5.5)$$

Use of the latter and eq. (3.9) furnishes the result (5.3).

Since nodes  $a$  and  $b$  communicate via node  $c$ , the remaining calculations are greatly simplified by choosing  $\mathbf{B}(c) = \mathbf{0}$ , whereupon eq. (3.12) directly furnishes the values of the remaining  $\mathbf{B}$  vectors,

$$\frac{\mathbf{B}(a)}{l} = \frac{2}{3} \left( \frac{w_{-x} - w_{+x}}{2w_y} \right) \mathbf{i}_x - \mathbf{i}_y, \quad (5.6)$$

$$\frac{\mathbf{B}(b)}{l} = \frac{2}{3} \left( \frac{2w_{+x} + w_{-x}}{w_x + w_{-x}} \right) \mathbf{i}_x, \quad (5.7)$$

which have been simplified with use of eq. (4.5).

Compute  $\tilde{\mathbf{b}}(j)$  from eq. (3.11), with use of eqs. (6.7) and (6.9), and use the result in eq. (6.5) to ultimately arrive at the dispersivity dyadic

$$\frac{\bar{\mathbf{D}}^*}{D} = \bar{D}_{xx}^* \mathbf{i}_x \mathbf{i}_x + \bar{D}_{yy}^* \mathbf{i}_y \mathbf{i}_y, \quad (5.8)$$

where the components of the dispersivity,

$$\frac{\bar{D}_{xx}^*}{D} = \frac{4}{27} \left[ \frac{(2w_{+x} + w_{-x})^2 + (2w_{-x} + w_{+x})^2}{(w_{+x} + w_{-x})^2} + \right], \quad (5.9)$$

$$\frac{\bar{D}_{yy}^*}{D} = \frac{2}{3}, \quad (5.10)$$

have been rendered in terms of the molecular diffusivity,  $D$ , with use of eq. (4.4).

Clearly, the lateral dispersivity,  $\bar{D}_{yy}^*$ , obeys the Nernst-Einstein relationship (1.2) for any choice of the transition parameters, as must be the case since there exists no bias in the lateral direction. In contrast, the axial dispersivity,  $\bar{D}_{xx}^*$ , only obeys the Nernst-Einstein relationship in the limit where  $w = 1/4$  ( $\forall j$ ), i.e. for pure molecular diffusion. Importantly,

the axial dispersion is also invariant to the arbitrary orientation of the  $x$ -axis. If one adopts the small-bias parameters (4.6), the axial dispersion reduces to the form

$$\frac{\bar{D}_{xx}^*}{D} = \frac{2}{3} + \frac{10}{27}\epsilon^2. \quad (5.11)$$

For finite field strengths, there exists a so-called ‘‘Taylor’’ contribution (or convective dispersivity) in the direction of the field, the latter depending quadratically upon  $\epsilon$ , or, equivalently, the square of the Peclet number. The latter result agrees with conventional continuum analyses of the convective dispersivity.

## VI. UNBIASED RANDOM WALK

### A. Simplification of the General Theory

Significant simplifications are realized when  $w(j) = w = \text{const.}$  ( $\forall j$ ), which is equivalent in its consequences to an unbiased random walk (or molecular diffusion) on the lattice, albeit with the possibility of rejected steps due to the presence of the obstacles. For a unit cell with  $\eta$  available sites, the asymptotic probability adopts the form

$$P_0^\infty(i) = \eta^{-1} \quad (\forall i), \quad (6.1)$$

reflecting the fact that it is equally likely for the particle to be located at any of the available sites [30]. With use of eq. (2.2), it is easily shown that eq. (6.1) satisfies eqs. (3.7)-(3.8). Substitution of eq. (6.1) into (3.6) reveals that

$$\bar{\mathbf{U}}^* = \left[ \frac{w}{\eta\tau} \right] \sum_{j \in E\Gamma_l} \mathbf{R}(j). \quad (6.2)$$

Since  $E\Gamma_l$  only contains edges entering the unit cell, the lattice structure guarantees that each edge possessing the macroscopic jump vector  $\mathbf{R}(j)$  can be paired with another edge whose macroscopic jump vector is  $-\mathbf{R}(j)$  (see, for example, Fig. 2). Consequently, the summation appearing in eq. (6.2) is identically zero, whereupon

$$\bar{\mathbf{U}}^* = \mathbf{0}, \quad (6.3)$$

as must be the case for a pure diffusion problem.

The  $\mathbf{B}$ -equation (3.12) undergoes a similar simplification in the unbiased limit,

$$\sum_{j \in \Omega^+(i)} [\mathbf{B}(i') + \mathbf{R}(j)] - \left[ \frac{1 - w(i)}{w} \right] \mathbf{B}(i) = \mathbf{0}. \quad (6.4)$$

The  $\tilde{\mathbf{b}}(j)$  are still computed by eq. (3.11), whereupon  $\bar{\mathbf{D}}^*$  adopts the form

$$\bar{\mathbf{D}}^* = \left[ \frac{w}{2\eta\tau} \right] \sum_{j \in E\Gamma_i} \tilde{\mathbf{b}}(j)\tilde{\mathbf{b}}(j), \quad (6.5)$$

For certain geometries, the present scheme for computing the effective diffusivity is computationally more efficient than the alternative procedure [16] of evaluating  $\bar{\mathbf{M}}^*$  in the low-force limit and then using eq. (1.2) to compute  $\bar{\mathbf{D}}^*$ . First, the coefficient matrix appearing in eq. (6.4) is invariant to spatial direction. Consequently, it is only necessary to specify the new solution vector in order to calculate a second (or third) component of  $\mathbf{B}$ . In contrast, the method of Ref. 16 requires computing a separate set of probabilities corresponding to the external force being oriented in each direction, each calculation (generally) involving a new coefficient matrix. While both methods require the same number of matrix inversions, the  $\mathbf{B}$  matrices are one dimension smaller. However, we expect this slight edge to be offset by the more involved calculations required to compute  $\bar{\mathbf{D}}^*$  by eq. (6.5). Importantly, though, the present method corresponds *exactly* to the case of no applied force, which eliminates the need to obtain the perturbation to the uniform probability distribution in the low-force limit, although this can be done fairly efficiently [5]. The Nernst-Einstein equation scheme is preferable, however, when significant geometrical simplifications can be effected by eliminating the macroscopic jump vectors and making use of “identical” nodes. That being said, both the present technique and the Nernst-Einstein limit technique are markedly less complicated than first-passage time analyses, and either method serves as an efficient analytical alternative to conventional simulation techniques, as well as a check on complex numerical codes.

## B. Pure Diffusion in an Asymmetric Array

As a final example, we compute the effective diffusivity of a particle moving on the lattice shown in Fig. 1. The effective diffusivity for this particular geometry was previously computed by Mercier *et al.* [16] using the techniques mentioned §I, and we demonstrate here that the present theory reproduces their results.

There are seven available locations in the unit cell,  $\eta = 7$ , and the jump probability is  $w = 1/4$ . The jump time,  $\tau$ , is given by the Brownian time scale of eq. (4.6). The probability of remaining on node  $i$  is equal to the number of adjacent unavailable sites divided by four,

$$w(i) = \begin{cases} 0, & i = b, c, d, f, \\ 1/4, & i = e, g, \\ 1/2, & i = a. \end{cases} \quad (6.6)$$

With the edge numbers depicted in Fig. 2, the macroscopic jump vectors are

$$\mathbf{R}(j) = 2l \begin{cases} 2\mathbf{i}_x, & j = 1, \\ -2\mathbf{i}_x, & j = 2, \\ -\mathbf{i}_y, & j = 3 - 5, \\ \mathbf{i}_y, & j = 6 - 8, \\ \mathbf{0}, & \text{otherwise.} \end{cases} \quad (6.7)$$

Substituting the relevant parameters into eq. (6.4) and choosing  $i^* = d$  (i.e.  $\mathbf{B}(d) = \mathbf{0}$ ),

$$\begin{aligned} & \begin{bmatrix} -2 & 1 & 0 & 0 & 0 & 0 \\ 1 & -4 & 1 & 2 & 0 & 0 \\ 0 & 1 & -4 & 0 & 2 & 0 \\ 0 & 2 & 0 & -3 & 1 & 0 \\ 0 & 0 & 2 & 1 & -4 & 1 \\ 0 & 0 & 0 & 0 & 1 & -3 \end{bmatrix} \cdot \begin{bmatrix} \mathbf{B}(a) \\ \mathbf{B}(b) \\ \mathbf{B}(c) \\ \mathbf{B}(e) \\ \mathbf{B}(f) \\ \mathbf{B}(g) \end{bmatrix} \\ & = -4l \begin{bmatrix} 1 \\ 0 \\ 0 \\ 0 \\ 0 \\ 0 \end{bmatrix} \mathbf{i}_x + 2l \begin{bmatrix} 0 \\ 1 \\ 1 \\ -1 \\ -1 \\ -1 \end{bmatrix} \mathbf{i}_y. \end{aligned} \quad (6.8)$$

The solution of this system of equations is

$$\begin{bmatrix} \mathbf{B}(a) \\ \mathbf{B}(b) \\ \mathbf{B}(c) \\ \mathbf{B}(e) \\ \mathbf{B}(f) \\ \mathbf{B}(g) \end{bmatrix} = \frac{l}{4} \begin{bmatrix} 11 \\ 6 \\ 3 \\ 5 \\ 3 \\ 1 \end{bmatrix} \mathbf{i}_x + l \begin{bmatrix} 0 \\ 0 \\ 0 \\ 1 \\ 1 \\ 1 \end{bmatrix} \mathbf{i}_y. \quad (6.9)$$

Compute  $\tilde{\mathbf{b}}(j)$  from eq. (3.11), with use of eqs. (6.7) and (6.9), and use the result in eq. (6.5) to furnish the dispersivity dyadic

$$\bar{\mathbf{D}}^* = \left( \frac{5}{28} \mathbf{i}_x \mathbf{i}_x + \frac{3}{14} \mathbf{i}_y \mathbf{i}_y \right) \frac{l^2}{\tau}, \quad (6.10)$$

or, in terms of  $D$ ,

$$\bar{\mathbf{D}}^* = \left( \frac{5}{7} \mathbf{i}_x \mathbf{i}_x + \frac{6}{7} \mathbf{i}_y \mathbf{i}_y \right) D, \quad (6.11)$$

The latter result agrees exactly with Ref. 16. Although not shown here, the present calculation scheme also reproduces the low-field mobilities obtained previously [16] during the course of the Nernst-Einstein calculation, although knowledge of the latter mobilities proves unnecessary to compute  $\bar{\mathbf{D}}^*$ .

Having furnished a third independent verification of the value of  $\bar{\mathbf{D}}^*$  for this array, we turn our attention to the volume-averaging theory [17] and investigate its comparable result. The pure diffusion problem includes no bias in the transition probabilities and results in zero mean velocity, whereupon their generic result for the  $yy$  component of the dispersivity adopts the form

$$\bar{D}_{yy}^* = \Gamma \left( 1 - \sum_W \hat{n}_y g^y \right) - v_y \sum g^y, \quad (6.12)$$

where  $\Gamma$  is their dimensionless diffusivity,  $\sum_W$  is the summation over all sites adjacent to the obstacle,  $\hat{n}_y$  are outward pointing normal vectors from the obstacles,  $\sum$  is the sum over all available sites,  $v_y$  is the microscopic drift velocity, and  $g^y$  is the volume-averaging quantity which plays a similar role to our  $\mathbf{B}$  field. Referring back to Fig. 1, the quantity  $v_y = 0$ , since the transport process only includes diffusion in the  $y$ -direction. Consequently, the second term in eq. (6.12) makes no contribution to the effective diffusivity. Moreover, only site  $a$  has a non-zero value of  $\hat{n}_y$ . Indeed, the latter site contains both a positive and negative unit

vector, corresponding to the lower and upper obstacle sites. As such, the summation  $\sum_W$  makes no contribution to  $\bar{D}_{yy}^*$ , and one recovers the physically incorrect result  $\bar{D}_{yy}^* = \Gamma = D$ .

## VII. CONCLUDING REMARKS

The present contribution has developed a generic scheme for computing the mean velocity vector,  $\bar{\mathbf{U}}^*$ , and dispersivity dyadic,  $\bar{\mathbf{D}}^*$ , from lattice models of transport in spatially periodic arrays of obstacles, the latter representing simple models of gel electrophoresis. To the best of our knowledge, this constitutes the only analytical method available at the present time for correctly computing the dispersivity dyadic from lattice Monte Carlo models for finite fields. The power and simplicity of the present calculation scheme renders it appropriate for revisiting the Ogston sieving problems considered previously [2, 3, 4, 5, 6, 7, 8, 9, 10]. in order to investigate the non-trivial solute dispersion arising during such transport processes.

Furthermore, it may be possible to use the general framework developed here to analyze DNA separations in microfluidic devices [11, 12, 13], provided that rational rules can be established for the transition probabilities prevailing therein. In the case of so-called rectified Brownian motion [11, 12, 21] (or vector chromatography [22]), a directional separation is achieved by applying the force at an angle with respect to the symmetry axes of the array. One should be able to analyze these devices in a manner similar to Ref. 17, although it is recommended that the present approach be employed to compute the dispersivity. It would be interesting to consider a mesh which is sufficiently fine in order to account for local variations in field strength and direction arising from the fact that the electric field does not penetrate the obstacles. The latter variations were recently demonstrated to have a strong effect on the experimental realization of directional separation schemes [23].

In the case of magnetosensitive arrays [13], the separation is achieved by a size-specific “hold-up” of the different DNA strands on the posts of the array. Consequently, application of the present scheme would require augmenting the hard-core repulsion of the obstacles to also account for the “attractive” residence time of the molecules when they become hooked. This problem is analogous to the inclusion of attractive forces exerted by the fibers of the gel [6], although exactly defining what is meant by the “attraction” to the posts is somewhat more ambiguous, since the attraction is not caused by a physical potential well.

## Acknowledgments

The author would like to thank Gary Slater of University of Ottawa for an enlightening discussion on Monte Carlo simulations. The encouragement of Jean-Louis Viovy of Institut Curie is greatly appreciated. This work was supported by a Postdoctoral Fellowship from Institut Curie.

---

- [1] N. G. van Kampen, *Stochastic Processes in Physics and Chemistry* (North-Holland, New York, 1981).
- [2] G. W. Slater and H. L. Guo, *Electrophoresis* **17**, 977 (1996).
- [3] G. W. Slater and H. L. Guo, *Electrophoresis* **17**, 1407 (1996).
- [4] G. W. Slater and J. R. Treurniet, *J. Chromatogr. A* **772**, 39 (1997).
- [5] J.-F. Mercier and G. W. Slater, *Electrophoresis* **19**, 1560 (1998).
- [6] J. Labrie, J.-F. Mercier, and G. W. Slater, *Electrophoresis* **21**, 823 (2000).
- [7] J. Boileau and G. W. Slater, *Electrophoresis* **22**, 673 (2001).
- [8] J.-F. Mercier and G. W. Slater, *Macromolecules* **34**, 3437 (2001).
- [9] J.-F. Mercier, F. Tessier, and G. W. Slater, *Electrophoresis* **22**, 2631 (2001).
- [10] M. G. Gauthier and G. W. Slater, *J. Chem. Phys.* **117**, 6745 (2002).
- [11] C. F. Chou, O. Bakajin, S. W. P. Turner, T. A. J. Duke, S. S. Chan, E. C. Cox, H. G. Craighead, and R. H. Austin, *Proc. Natl. Acad. Sci. U.S.A* **96**, 13762 (1999).
- [12] M. Cabodi, Y.-F. Chen, S. W. P. Turner, H. G. Craighead, and R. H. Austin, *Electrophoresis* **23**, 3496 (2002).
- [13] P. S. Doyle, J. Bibette, A. Bancaud, and J.-L. Viovy, *Science* **295**, 2237 (2002).
- [14] J. Koplik, *J. Fluid Mech.* **119**, 219 (1982).
- [15] J. C. Giddings, *Unified Separation Science* (Wiley and Sons, New York, 1991).
- [16] J.-F. Mercier, G. W. Slater, and H. L. Guo, *J. Chem. Phys.* **110**, 6050 (1999).
- [17] C. Keller, F. Marquardt, and C. Bruder, *Phys. Rev. E* **65**, 041927 (2002).
- [18] P. M. Adler and H. Brenner, *PhysicoChem. Hydrodyn.* **5**, 269 (1984).
- [19] K. D. Dorfman and H. Brenner, *Phys. Rev. E* **65**, 021103 (2002).

- [20] G. W. Slater, J. Rousseau, and J. Noolandi, *Biopolymers* **26**, 863 (1986).
- [21] T. A. J. Duke and R. H. Austin, *Phys. Rev. Lett.* **80**, 1552 (1998).
- [22] K. D. Dorfman and H. Brenner, *J. Colloid Interface Sci.* **238**, 390 (2001).
- [23] L. R. Huang, P. Silberzan, J. O. Tegenfeldt, E. C. Cox, J. C. Sturm, R. H. Austin, and H. Craighead, *Phys. Rev. Lett.* **89**, 178301 (2002).
- [24] In free solution, these dyadics are isotropic and the solute mobility reduces to its Stokes mobility.
- [25] The zero-field limit dispersion coefficient is often referred to as the diffusion coefficient for the system, which should not be confused with the molecular diffusivity of the solute. For clarity, we will only use the term diffusion in the context of local motion and the term dispersion (or effective diffusion) in the context of averaged global motion.
- [26] By an unbiased walk, we mean that all jumps are equally likely at a given lattice site, but where some of the jumps may be rejected by the presence of the obstacles. In contrast, for a biased random walk, the likelihood of making a jump in a particular direction is biased by the presence of the imposed force, resulting in a preferred direction of motion. Jumps onto sites occupied by the obstacles are still rejected in the biased random walk.
- [27] For those edges contained entirely in unit cell  $\mathbf{I}$ ,  $\mathbf{I} = \mathbf{I}'$ .
- [28] In the context of the original discrete Taylor-Aris dispersion theory [19], it is possible to account for the rejected jumps by adding loops to the graph which return the particle to its original position. This alters the form of the master equation [cf. eq. (2.5)], requiring an additional sum over the outlet edges in  $\Omega^-(i)$ . Since the underlying logic of the lattice random walk is that the particle must make a jump at each time step (albeit with the possibility that this jump will be rejected), the resulting calculation scheme is greatly simplified by requiring a unitary probability [cf. eq. (2.2)] of jumping and accounting for rejected jumps by the factor  $w(i)$ .
- [29] It is expected that moving from a finite-difference approximation to a continuous derivative reflects the physical process being modeled, since the lattice model merely represents a discrete approximation to a continuous process.
- [30] When using the Nernst-Einstein relationship (1.2) to compute the effective diffusivity in the zero-field limit, the presence of an infinitesimally small force induces a bias in  $P_0^\infty$ . (As an illustrative example, consider the effect of curved field lines [9].) The latter bias appears here

only in the  $\mathbf{B}$ -field, since the force is identically zero.